International Journal of Nanoelectronics and Materials
Volume 15, No. 4, October 2022 [353-366]

Sol gel synthesis and characterization of porous nanosized oxide 70TiO_2-30 MgO film for anode solar cell application

Marwa M. Toraya[1], Doaa M. Atia[1*], Amany M. El Nahrawy[2], Ninet M. Ahmed[1], Saleh Hussin[3]

[1]Photovoltaic Cells Department, Electronics Research Institute (ERI), Cairo, Egypt
[2]Solid-State Physics Department, Physics Research Division, National Research Centre, 33 El-Bohouth St., Dokki, 12622, Egypt
[3]Electronics and Communications Engineering Department, Faculty of Engineering, Zagazig University, Egypt

Received 28 November 2021, Revised 22 April 2022, Accepted 13 June 2022

ABSTRACT

This work reports the infusion effect of Mg into TiO_2 nanocomposite for DSSC photo-anode application. TiO_2-MgO Porous nanosized structure oxide film was obtained using sol-gel technique at 400°C. The fabricated film is described in terms of crystallinity and morphology by XRD and HR-SEM. The fabricated thin-film demonstrated the structure of a semi-crystalline ($Ti_{2.94}Mg_{0.06}O_5$) and Ti_9O_{17} nanoparticle. SEM exhibited a smooth surface with crystalline nature, which matched with the crystallites size that estimated from XRD analysis and can be utilized as the large efficiency of the solar cells. The optical spectra showed that porous nanosized 70TiO_2-30MgO film band gap is 2.5 eV. XRD and optical results suggested that the insert of MgO in TiO_2 film compellingly improved the TiO_2 anode thin films.

Keywords: Nanosized Mg-doped TiO_2 thin films; photoanode; DSSC; Sol-gel Method; optical properties

1. INTRODUCTION

In the exploration for alternative, renewable, clean, and economical energy sources, solar cells are a competitive sort of device that yields solar energy and liberate electrical energy. Dye-sensitized solar cells (DSSC) as a type of various solar cells are attractive because of their characteristics such as easy formation, cheaper, and renewability [1]. DSSCs are an outstanding member of the larger group of thin film photovoltaic and DSSC should play a major role in the future of solar energy. DSSCs is one of the third generations of semiconductors-solar cells designed through photo-sensitized electrode (anode), and another one is a counter electrode (cathode) which fabricates a photoelectrochemical arrangement [2]. To yield higher efficiency, some parameters like light absorption and electron injection should be improved. The process of doping certain semiconductors (TiO_2, ZnO, SiO_2, AlO_2, CdO) with a foreign ion to reduce lattice bandgap is very efficient for increasing electron injection [3]. TiO_2 is a semiconductor material used for photo-anode due to its higher transparency, low cost, high availability, high stability, nontoxicity [4]. Because of TiO_2's excellent optoelectronic, wide band-gap semiconducting materials, it is one of the best choices for different solar energy applications [5]. Nano-TiO_2 as DSSC anode also consider as multi-functional material tenders like air and water purification over the employment of solar energy [6, 7].
TiO_2 photochemical features work to convert the solar radiations to efficient energy as in photovoltaic performer and hence encountering a higher deal of consideration. However, solar

* Corresponding author: doaa@eri.sci.eg

spectrum utilization has been restricted with a large bandgap of TiO_2 (3.2 eV) [8], thus most of TiO_2-efficiency can be enhanced through morphological adjustments or by introduction of various non-metals and metals components within the TiO_2 framework [9, 10]. The quality of the film and their physical-chemical properties can be improved, the introduction of metal ions is expected to perform a significant part in altering the catalytic activity, the charge carriers contents of the metal oxide ground, the crystallites size, surface potential, phase composition, and so on [11, 12]. Photo activities in photo anode can be improved by doping an alkaline earth metallic material like Magnesium, Mg into TiO_2 anatase [13]. In addition to enhance the optical properties and preventing the energy migration among TiO_2 ions in TiO_2 anode, it is necessary to introduce some modifications as Mn and Mg centres in the TiO_2 matrix [14]. MgO is considering the finest one in the chains, which can modified for the Ti in their bulk because of its ionic radius. Introducing MgO will not alter the crystal assembly. Several methods are approved to form a TiO_2-MgO film such as electrical beam evaporation, Chemical Vapor Deposition (CVD), sputtering, and sol gel. The sol-gel technique has been developed as a widely fabrication method in the last decades by researchers, thus sol-gel technique is adopted here due to several benefits such as the processing can be completed at low temperatures, easy, simple, and cheap. By applying this technique, it is common that the reactant sols are maintaining nanoparticles in a dispersed state within the applied solvents, which successively formed the sol. Further, these colloidal particles can be linked together by condensation to get the gel [15][16].

Table 1 presents a list of previous works used TiO_2 as a photoanode in their works. Moreover, using various materials as dopants to achieve the photoanode performance and efficiency of the cell are shown. In addition, the methods of fabrication used affected the final performance so it is recommended to focus on it in our work.

Table 1. The relative previous works of TiO_2 photo-anode

Material Used	Synthesis Method	Reference No.
Sm^{3+}/ Gd^{3+} doped TiO_2	Hydrothermal synthesis technique	[17]
Cu/Mn doped TiO_2	Microwave assisted hydrothermal method	[18]
TiO_2	Flame spray pyrolysis and hydrothermal Sol-Gel	[19]
Ni/Zn Co-doped TiO_2	Spin-Coating Sol–Gel Technique	[20]
Al doped TiO_2	Sol-Gel Technique	[21]
Ag doped TiO_2	Sol-Gel Technique	[22]
MgO doped TiO_2	Spin-Coating Sol–Gel Technique	[23]

The aim of this study was concentrated on a pure TiO_2 photo-anode in DSSC replaced by a composite of 70TiO_2-30MgO. This composite was prepared using spin coating sol–gel technology. The prepared composite was deposited on glass substrate, and the deposited thin films were calcinated in air at 400 ^oC for 1 hr to achieve a porous 70TiO_2-30MgO layer. The effect of Mg metal on the matrix of TiO_2 has been studied by structural characterization (XRD&SEM) on these films, as well as their optical properties.

2. EXPERIMENTAL WORK

The preparation and characterization of 70TiO_2-30MgO photo-anode based on spin coating sol-gel method will be described in the following sections. In the following section, the materials used, the method of preparation are also discussed. The characterization of the prepared films using XRD, SEM and UV-VIS-NIR are discussed in details.

2.1 Preparation of 70TiO_2-30MgO Anode

The 70TiO_2-30MgO thin films were dropped using sol-gel spin coating method. It started with clean the 2x2 cm^2, 1.1mm thick glass substrate in ultrasonic by immersing it in acetone, followed by washing using distilled water, then the substrates were dried for 5 min at 50°C on hot plate in air before the deposition [5]. The flow chart shown in Fig 1 illustrates that the 70TiO_2-30MgO were synthesized using Titanium Isopropoxide Ti $[OCH(CH_3)_2]_4$ (TIP) and Magnesium nitrate-hexahydrate ($Mg(NO_3)_2{\cdot}6H_2O$), which are used for thin film deposition without additional purification. At first, Magnesium nitrate-hexahydrate is dissolved in a mixture of citric acid and distilled water after putting them in magnetic stirring for vigorous stirring. Then, Titanium Isopropoxide is dissolved in 15 ml of acetyl acetone and a mixture of a citric acid and distilled water, after that the synthesized Titanium Isopropoxide Ti $[OCH(CH_3)_2]_4$ and Magnesium nitrate-hexahydrate ($Mg(NO_3)_2{\cdot}6H_2O$) are mixed and stirred vigorously for 2 hr in magnetic stirring to obtain Titanium Magnesium solution (TM). The prepared solution is aged for 24 hr in room temperature to obtain the suitable viscosity. The TM solution deposited on glass substrates by using sol-gel - spin coating technique at 1500 rpm for 30 s. The prepared TM thin films will be obtained by drying them using a hot plate at 70 ^oC in air after each layer deposition to evaporate and remove residual solvents and this step are repeated five times to obtain the desired thickness. Finally, the promising 70TiO_2-30MgO thin film is calcined at 400 ^oC for 1 hr. From here, the (TM) semiconductors thin film is ready for all characterization process.

2.2 Characterization of 70TiO2-30MgO Anode Film

The XRD patterns of the promising sensitized (TM) thin film was achieved by Bruker D8 from Germany equipped with CuKα (λ = 1.54 A^o) in the 2θ range of 10°– 80° and operating at 40 kV and 40 mA. Also, the XRD profile of semi-crystalline film was refined by the profile parameters using FullProf software (the pseudo-Voigt fitting model) and VESTA-win64 software [24].

The surface morphology of the synthesized 70TiO_2-30MgO thin film was studied using Scanning Electron Microscopy (SEM), Hitachi S4800, Japan, energy dispersive X-ray EDXRF (Shimadzu EDX-7000). Analysis was performed to determine the concentration of elements and the contaminants in the film. The optical properties of the film were measured using a UV-VIS-NIR spectrophotometer (Shimadzu-2540) in the wavelength range of 300-1000 nm.

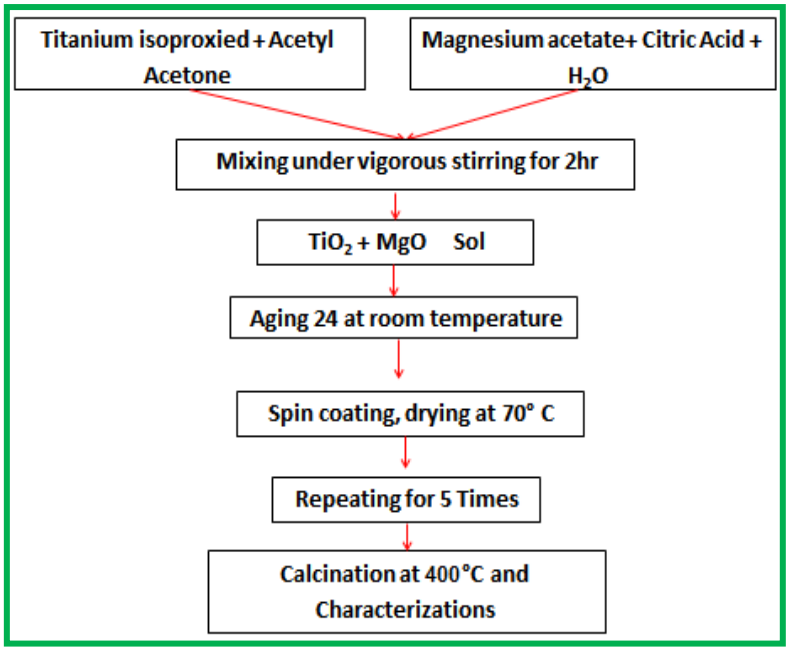

Figure 1. Flow chart of synthesis procedure of 70TiO_2-30 MgO anode film

3. RESULTS AND DISCUSSIONS

In this section, the structure and optical properties of 70TiO_2-30 MgO anode film will be discussed.

3.1. Structural Evaluation (X-Ray Diffraction)

The X-ray diffraction pattern of porous nanosized 70 TiO_2-30 MgO thin-film obtained by sol-gel method and dropped at glass substrate using spin coating is shown in Fig. 2(a). The obtained XRD shows that the deposited film has a semi-crystalline structure and exhibited main peaks at 8.8°, 11.3°, 25.17°, 31.48°, 42°, and 61.62° respectively according to JCPDS card (No. 82-1136) monoclinic magnesium titanate oxide ($Mg_{0.06}Ti_{2.94O5}$) and anorthic titanium oxide (Ti_9O_{17}) card (No. 85-1061) and the main peak at 31.48°.

Generally, the lower intensity of the peaks and the formation of Ti_9O_{17} phase are formed as a second phase when calcination 70 TiO_2-30 MgO anode film at a lower temperature [25]. It is known that the Mg_2TiO_4 matrix is unstable at low temperatures and may suffer from decomposition to TiO_2 and MgO [26]. Herein, TiO_2-MgO binary nanosized oxide was synthesized by the sol-gel processing [27] caused in a homogeneous sol, through slow rate solvent evaporation leading the gelation occurred at low temperature [28]. A highly porous TiO_2-MgO oxide film with a high surface area was probably owing to the formation of a new magnesium-titanium phase where the nanoparticles can disturb the finest pores of the TiO_2-MgO system. Scherrer's equation was exercised to calculate the crystallite size, D [29]:

$$\left(D = \frac{(0.9\,\lambda)}{(\beta\cos\theta)}\right) \quad (1)$$

where, Θ is the Bragg's-angle, the full width at half maximum (β) in radians and λ is the X-ray wavelength. The crystallite size (D) of porous nanosized 70 TiO_2-30 MgO thin-film is calculated to be 21 nm at the principle peak (112).

The semi-crystalline structure for TiMg film was is confirmed using FullProf-software, as shown in Fig. 2(b, c). Monoclinic (P 2/c) $MgTiO_2$ phase was to obtain the Rietveld parameters, where a=4.51676 A^o, b=5.50314 A^o, c=4.88603 A^o, and the cell volume (V) =121.4429 A^o.

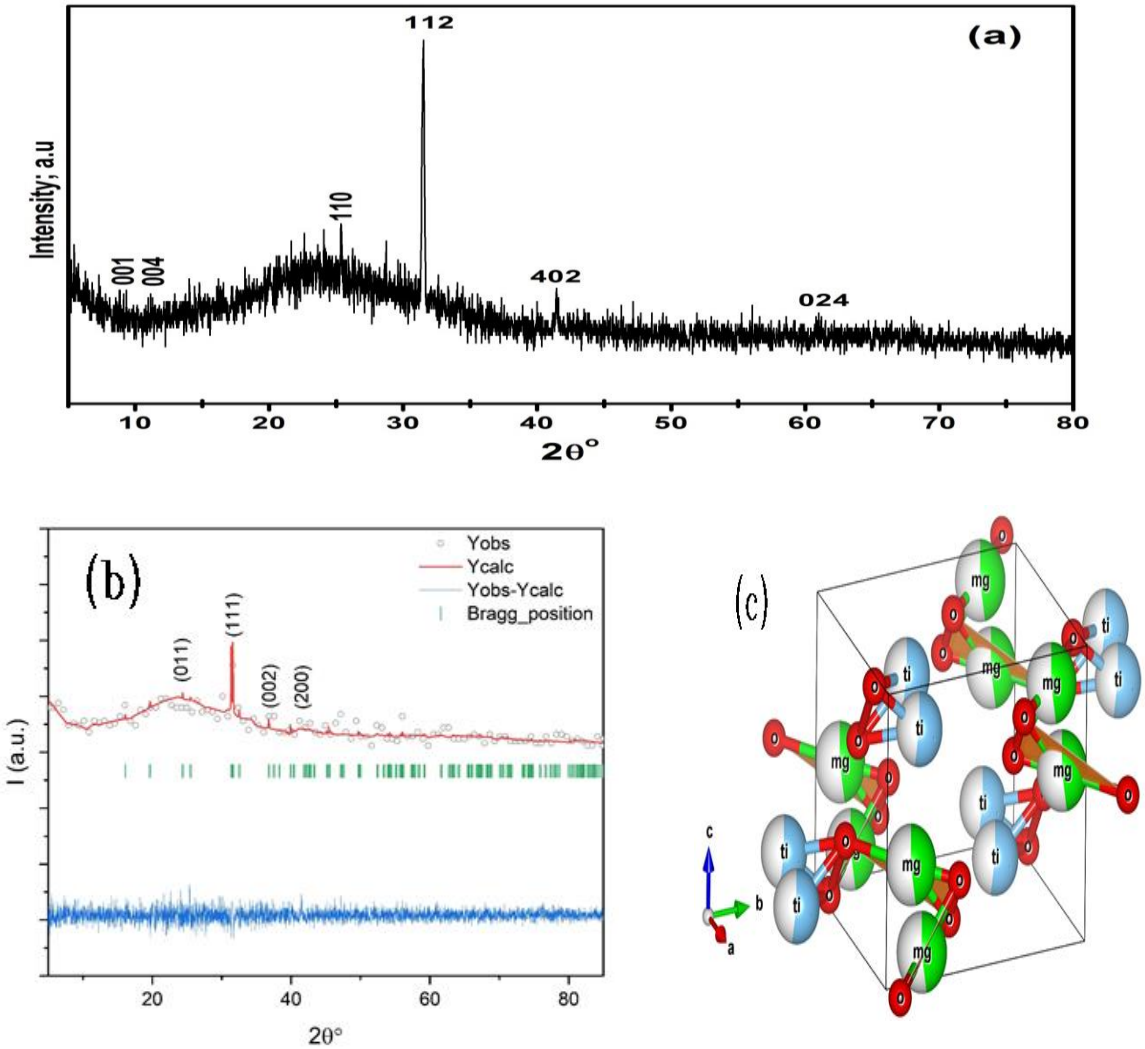

Figure 2. (a) XRD pattern of 70TiO_2-30 MgO anode film, (b) FullProf XRD pattern and (c) Configuration of 70TiO_2-30 MgO structure

3.2. Films Morphology (SEM/EDX)

The morphology characterization using Scanning Electron Microscopy (SEM) at 20 Kv is illustrated in Fig. 3. The images confirmed the smooth surface for porous nanosized 70TiO_2-30MgO anode film surface synthesized by sol-gel method. Very dense and uniform micrographs of the anode film annealed at 400 ^{o}C with an average diameter of 24.9 nm are achieved.

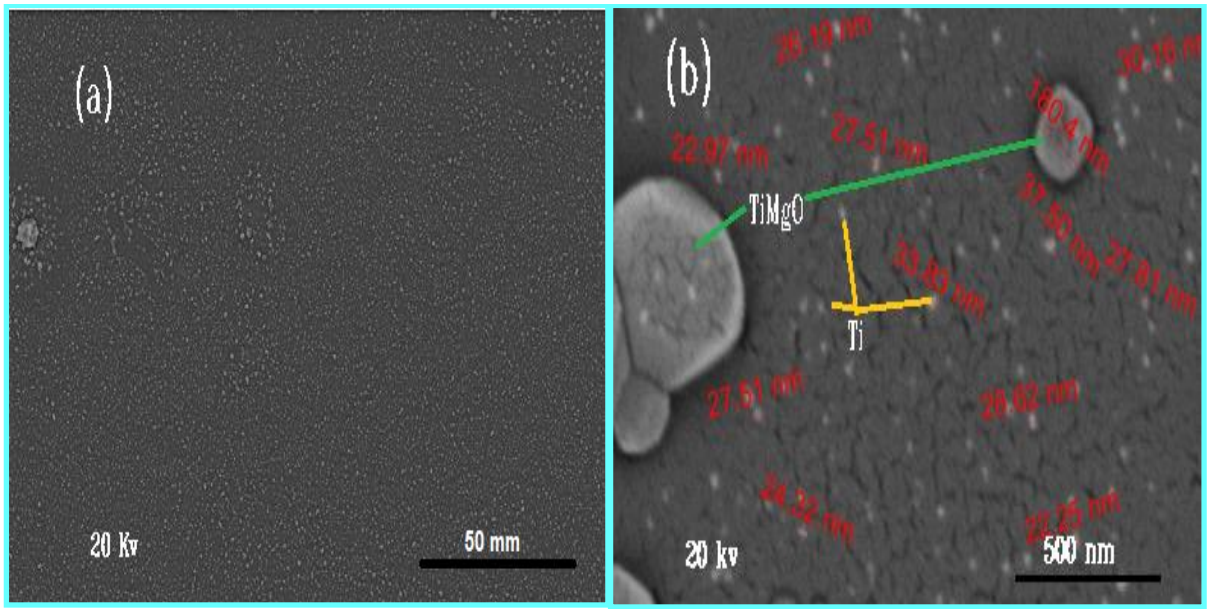

Figure 3. Surface morphology of 70TiO_2-30 MgO anode film

3.3. Optical properties of oxide 70TiO_2-30 MgO porous nanosized anode film

UV – Vis spectrophotometer is used to scrutinize the optical properties of the synthesized porous nanosized oxide70TiO_2-30 MgO anode film calcined at 400 °C. The transmission spectrum for anode thin film in the wavelength range (300- 1000 nm) is shown in Fig. 4. The transmittance increases with increasing wavelength (λ) and attains optical transparency over 85% in the visible range. Fig. 5 depicts the reflection spectrum of TM thin film. The reflection reduces with increasing wavelength.

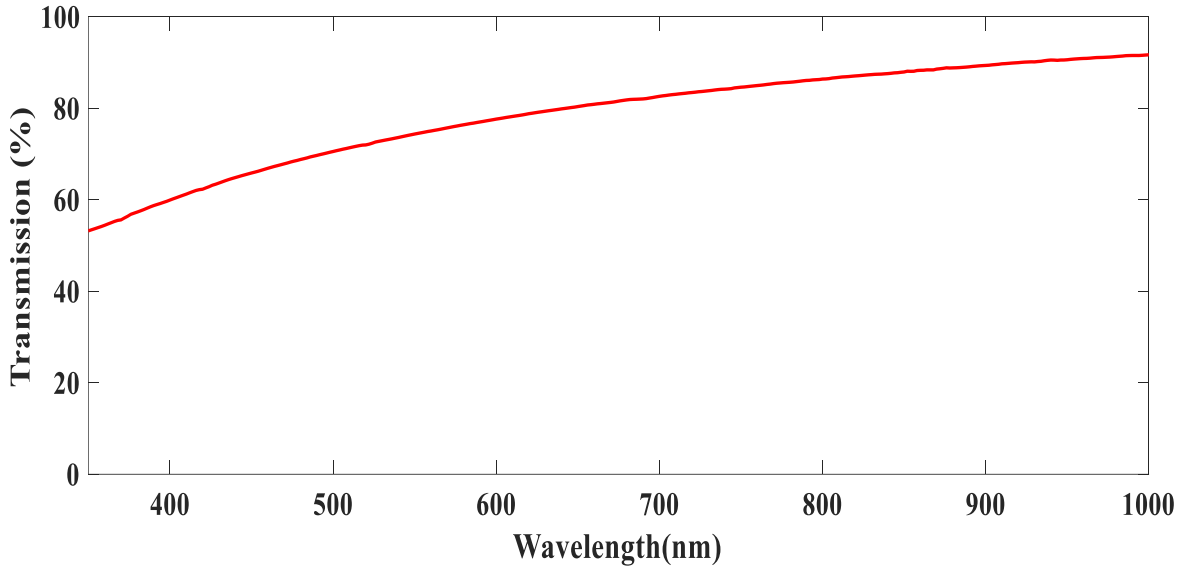

Figure 4. The transmission spectrum of 70TiO_2-30 MgO anode film

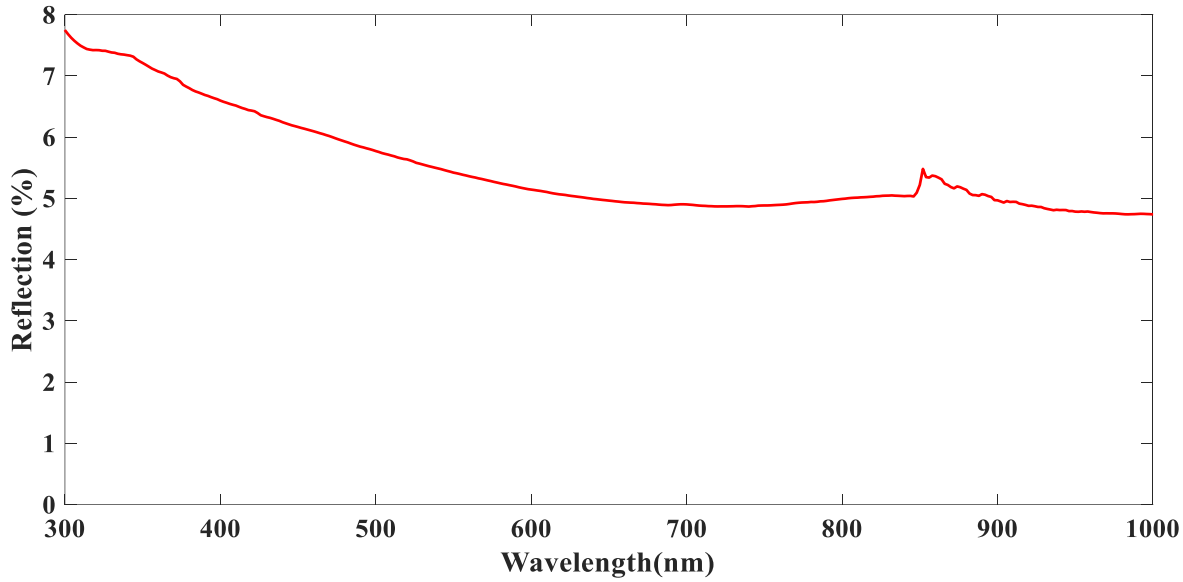

Figure 5. The reflection spectrum of 70TiO_2-30 MgO anode film

The absorption coefficient deliberated using Lambert law [30] of 70TiO_2-30MgO anode film is shown in Fig. 6:

$$\alpha = \frac{\ln\left({}^{1}/_{T}\right)}{t} \tag{2}$$

where 'T' is the transmittance and 't' is the film thickness.

It is observed that the absorption coefficient is high at a lower wavelength and decreases gradually at a higher wavelength. The calculated values of the absorption coefficient are in the order of 104 cm^{-1}.

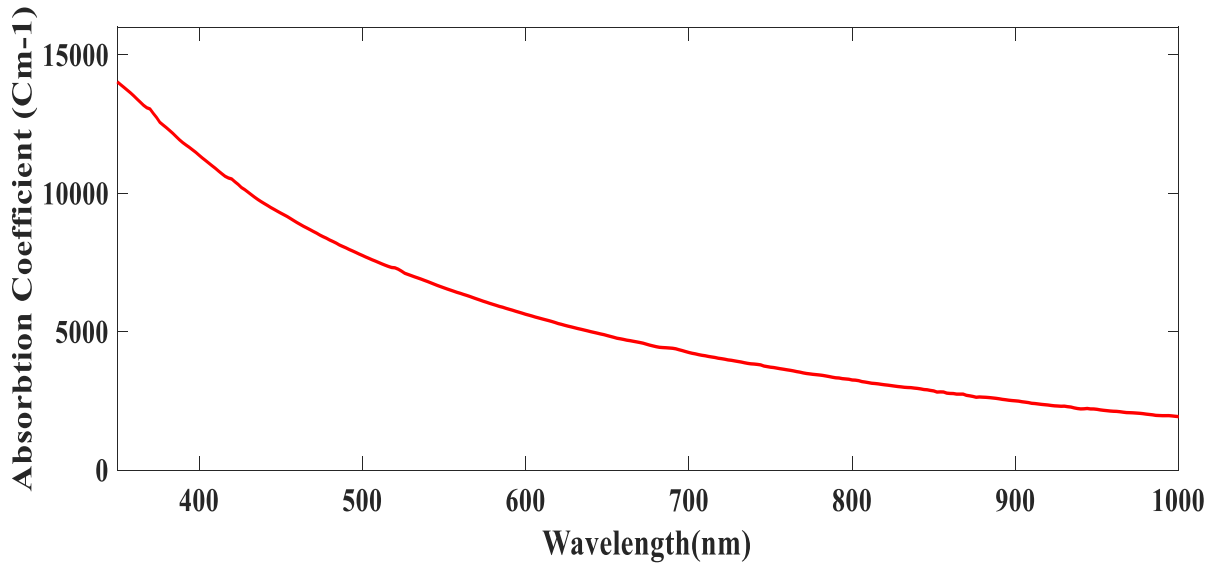

Figure 6. Absorption coefficient of 70TiO_2-30 MgO anode film

The bandgap of 70TiO_2-30 MgO anode film was estimated using the Tauc relation [31, 32] :

$$(\alpha h\vartheta)^2 = A(h\vartheta - E_g) \quad (3)$$

where α is absorption coefficient, h is Planck's constant, A is constant, ν is frequency of light radiation, and Eg is bandgap energy. The bandgap energy was determined via plotting $(\alpha h\upsilon)^2$ vs. hυ. The value of the bandgap of the film was obtained by extrapolation of the linear region of the plots of $(\alpha h\upsilon)^2$ to its intersection with the energy axis (hυ). The energy band gap of this sample is 2.5 eV (Fig. 7). It is in good agreement with the value reported elsewhere [33].

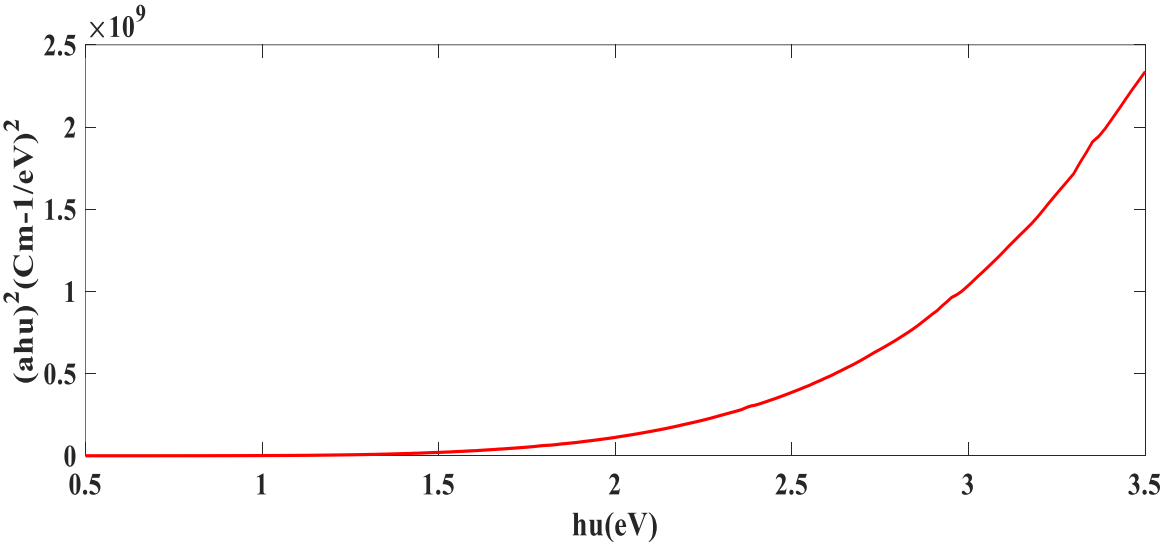

Figure 7. The plots of $(\alpha h\upsilon)^2$ vs. photon energy of 70TiO_2-30 MgO anode film

The extinction coefficient (k) of 70TiO_2-30MgO anode film was calculated using the expression:

$$K = \frac{\alpha\lambda}{4\pi} \quad (4)$$

Fig. 8 illustrated the variation of extinction coefficient with wavelength. We perceive that the extinction coefficient drops with an increase in wavelength.

Also, the refractive index (n) of the prepared film can be expressed in terms of the reflection (R) and the extinction coefficients (k) according to the Fresnel equation:

$$n = \frac{1+R}{1-R} + \sqrt{\frac{4R}{(1-R)^2} - K^2} \quad (5)$$

Fig. 9 appeared the decrease in refractive index (n) value of the 70TiO_2-30 MgO thin film with increasing wavelength in normal dispersion region. This conduct might be accredited to various oscillator modes in the semi-crystalline film.

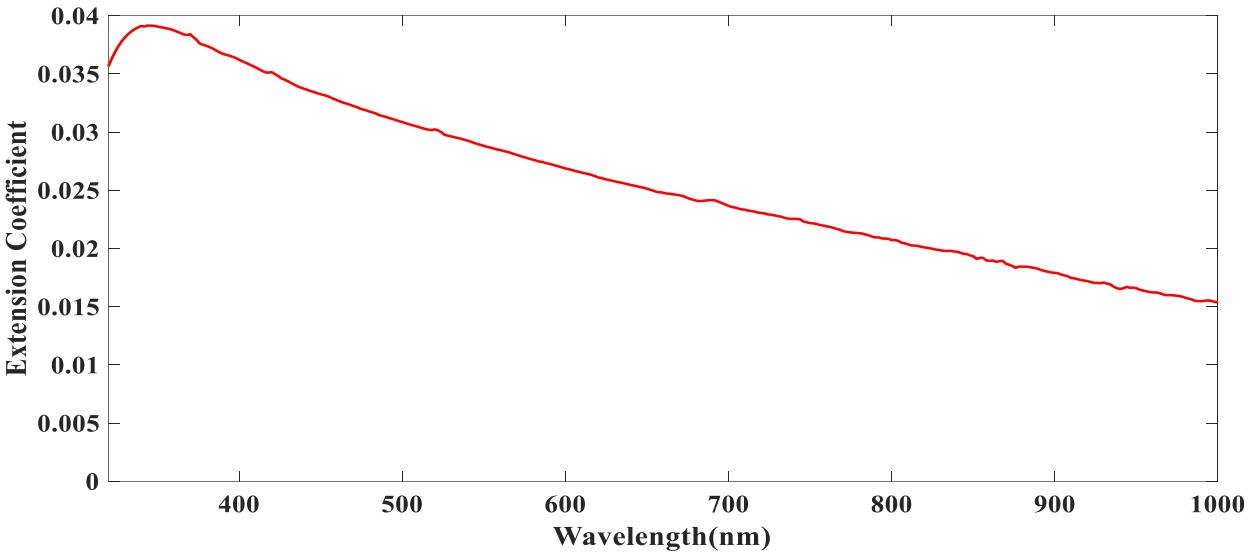

Figure 8. The extinction coefficient variation with wavelength of 70TiO_2-30 MgO anode film

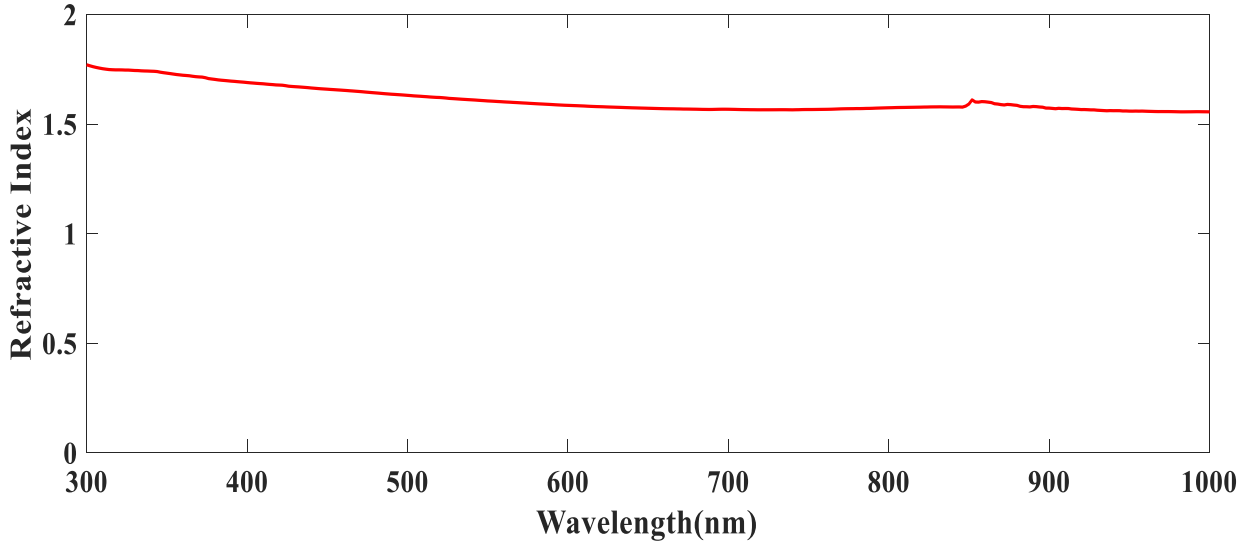

Figure 9. The refractive index variation with wavelength of 70TiO_2-30 MgO anode film

The estimated dielectric function is an essential intrinsic property and a complex extent of the thin film, which involves both the imaginary parts (ε_i) and the real (ε_r). The ε_r indicates how the rapidity of light in the film can be reduced down, however, the imaginary part transactions with the absorption of (hυ) by a dielectric system from the applied electric field owing to the dipole motion.

The estimated dielectric function of the deposited nanosized 70TiO_2-30MgO anode film was intended using the expression:

$$\varepsilon_T = \varepsilon_r + \varepsilon_i \quad (6)$$

Real and imaginary fragments of the dielectric constant (ε_T) are linked to the (n) and (k) values. The εr and εi values were calculated using these formula [34]:

$$\varepsilon_r = n^2 - K^2 \quad (7)$$

$$\varepsilon_i = 2\,n\,K \quad (8)$$

Fig. 10(a, b) illustrates the variation of εr (Dielectric Constant) and εi (Dielectric Loss) with wavelength. The values of ε_r and ε_i of the nanosized film decrease with incident photon wavelength. The real part of the dielectric constant spectrum is characterized by the presence of the peak at 350 nm may be attributed to a crystalline degree in the film. We see that the behaviour of the real dielectric constant (ε_r) is nearly similar to the refractive index (n) and the behaviour of (ε_i) with photon wavelength is nearly similar to the extinction coefficient and the values of (ε_r) are higher than that of (ε_i).

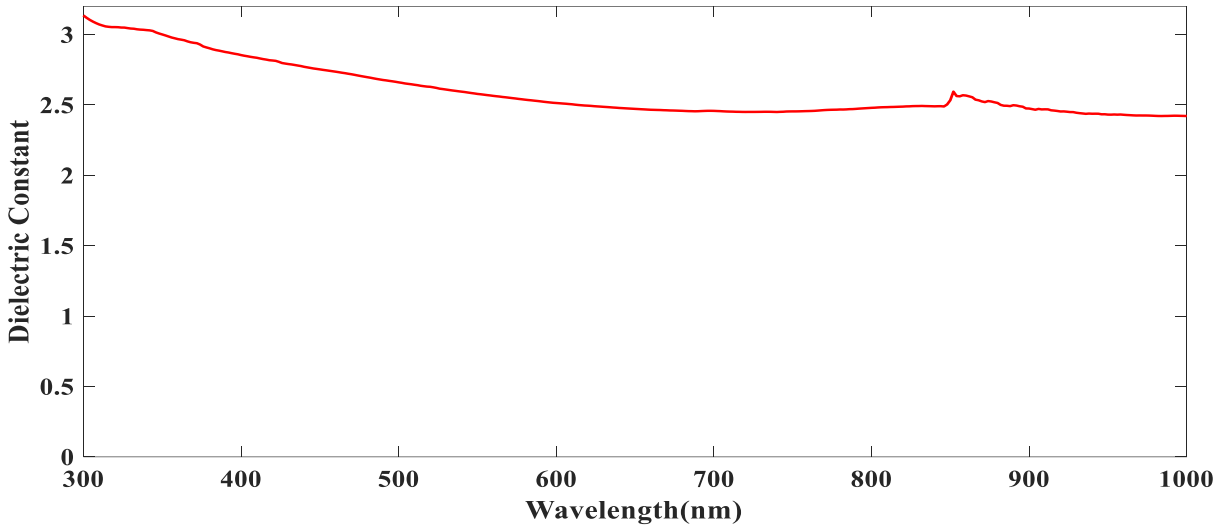

(a)

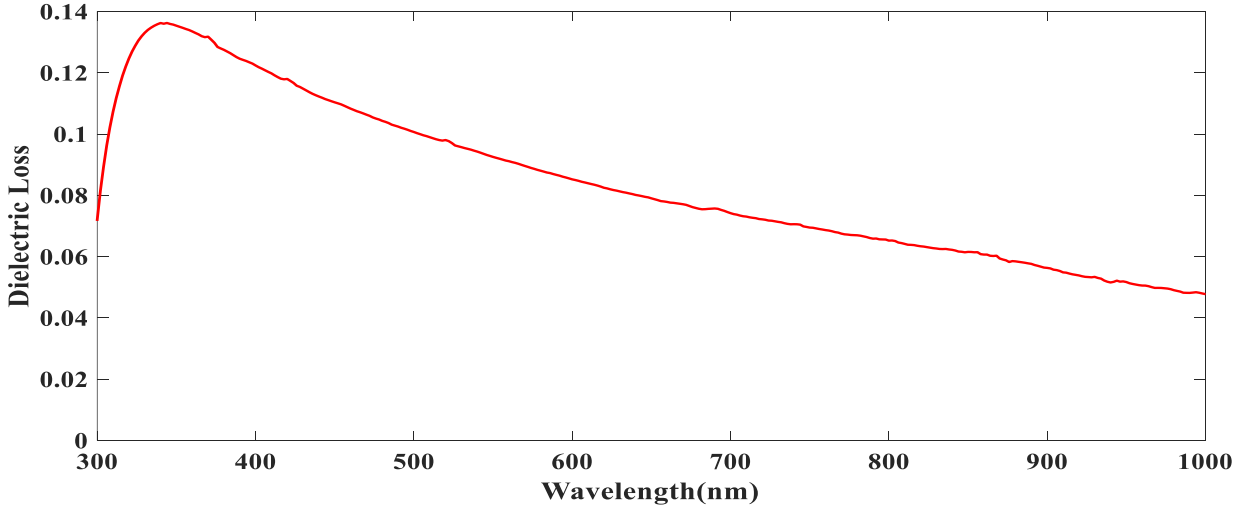

(b)

Figure 10. Variation of (a) real and (b) imaginary parts of the dielectric constant of the 70TiO_2-30MgO anode film

The expressions of optical conductivity (σ_{opt}) are mainly concerned with the study of the optical response for any material; also, the energy band structure of the deposited film is closely related to the optical conductivity. The optical conductivity of 70TiO_2-30MgO anode thin film can be calculated by using the absorption coefficient (α) as in the following equation:

$$\sigma_{opt} = \frac{\alpha nc}{4\pi} \qquad (9)$$

where n is the refractive index and c is the velocity of light. Fig. 11 demonstrates the optical conductivity variation as a function of photon wavelength. This behaviour can be attributed to the optical conductivity decreasing with an increase in wavelength also, the absorbance decreasing with an increase in wavelength.

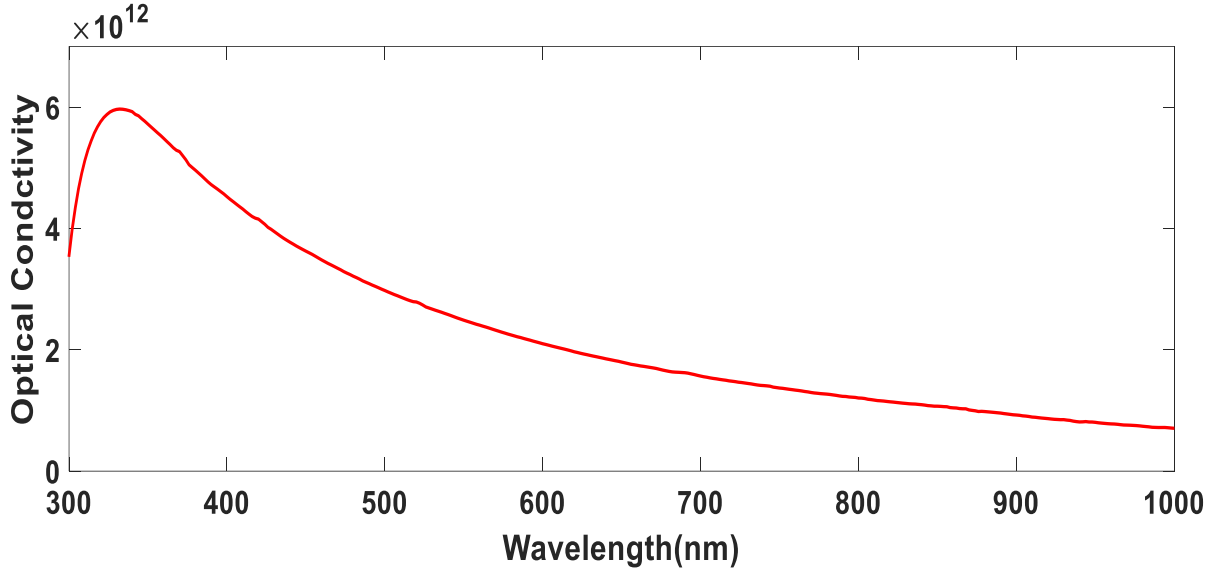

Figure 11. The optical conductivity variation with wavelength of 70TiO_2-30MgO anode film

The dielectric loss tangent (tan δ) of 70TiO_2-30MgO thin film, which represents how the electric energy dissipated into thermal energy and can be defined by the following relation:

$$tan\delta = \frac{\varepsilon i}{\varepsilon r} \tag{10}$$

where δ is the phase angle between the electric field and the polarization of the dielectric, ε_r and ε_i are the real and imaginary parts of the dielectric constant, respectively. The dielectric loss tangent of 70TiO_2-30MgO thin film variation with photon wavelength is shown in Fig. 12. It can be seen that the loss tangent decreases with increasing the photon wavelength and the change in the tan δ is dominated by the variation of ε_i.

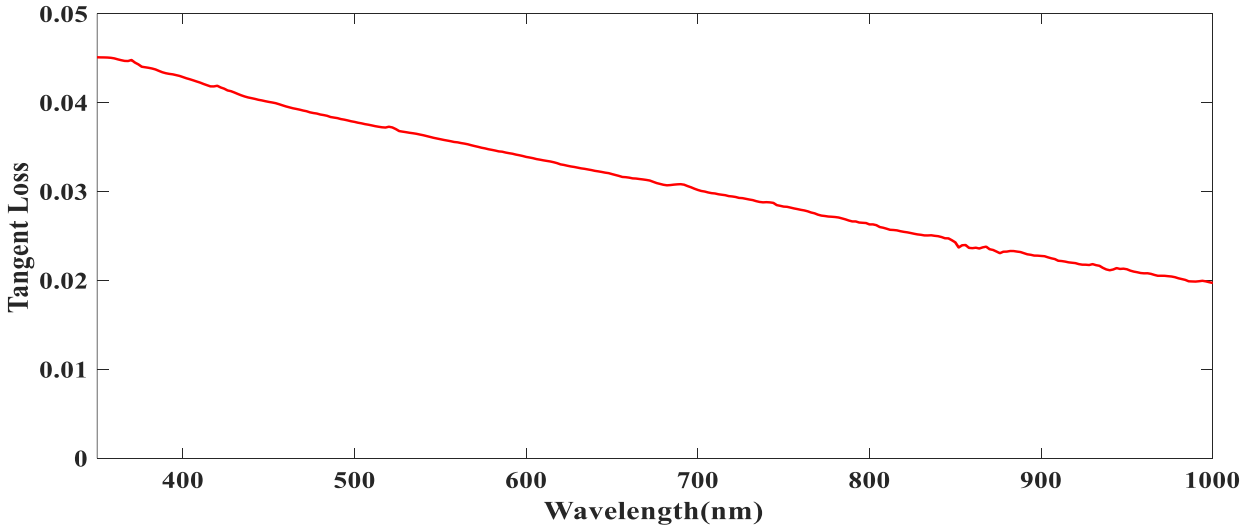

Figure 12. The tangent loss variation with wavelength of 70TiO_2-30MgO anode film

The Q-factor of 70TiO_2-30MgO thin film can be calculated from tangent losses which the quality factor Q is reciprocal of dielectric loss tangent by using the following equation:

$$Q = \frac{1}{\tan\delta} \tag{11}$$

The dependence of quality factor of 70TiO_2-30MgO thin film on photon wavelength is demonstrated in Fig. 13. It can be seen that the quality factor of 70TiO_2-30MgO thin film increase with increasing the photon wavelength and this proves that the material with lower εr generally has a higher Q value.

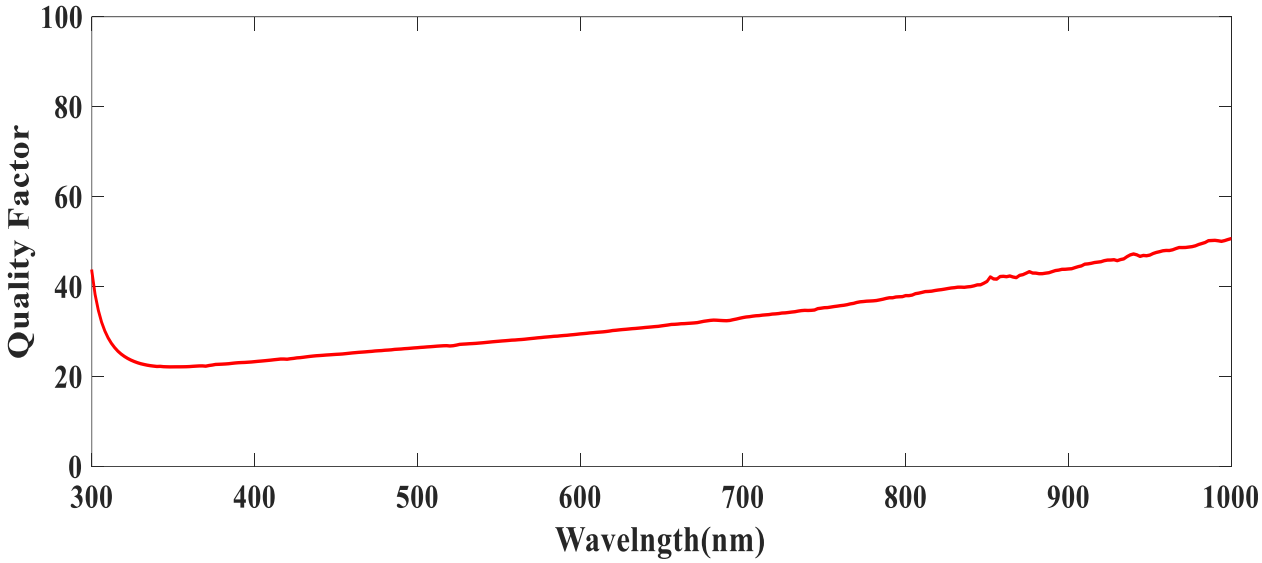

Figure 13. The quality factor variation with a wavelength of 70TiO_2-30MgO anode film

4. CONCLUSION

70TiO_2-30MgO thin film was magnificently prepared by the sol-gel method. Structural and optical properties of the prepared porous nanosized thin films were investigated. The transmittance of the synthesized films exceeded 85 % in the visible range. The bandgap for 70TiO_2-30MgO was estimated to be 2.5 eV, which is in good agreement with the reported value in the literature. The accidental distribution of the formed grains makes the film surface irregular and increased the light scattering sufferers at the interface. Illustrated low bandgap, high absorption may be suitable for different photovoltaic applications. Studying alternative dopants and dopant percentages effect on the TiO_2 properties will be considered in future.

References

[1] Y. . W. J. Wu, Z. Lan, J. Lin, M. Huang, Y. Huang, L. Fan, G. Luo, Y. Lin, Y. Xie, "Counter electrodes in dye-sensitized solar cells," *Chem. Soc. Rev.*, pp. 5975–6023, 2017, doi: 10.1039/c6cs00752j.

[2] S. Sathyajothi, R. Jayavel, and A. C. Dhanemozhi, "The Fabrication of Natural Dye Sensitized Solar Cell (Dssc) based on TiO2 Using Henna And Beetroot Dye Extracts," *Mater. Today Proc.*, vol. 4, no. 2, pp. 668–676, 2017, doi: 10.1016/j.matpr.2017.01.071.

[3] M. Safaei, "The International Debate on Preparation of Mg-Doped Tio2 Nanoparticles for Dye-Sensitized Solar Cell Applications," *J. Clin. Pathol. Lab. Med.*, vol. 1, 2020.

[4] W. Rho, D. H. Song, H. Yang, H. Kim, and B. S. Son, "Recent advances in plasmonic dye-sensitized solar cells," *J. Solid State Chem.*, vol. 258, no. October 2017, pp. 271–282, 2018, doi: 10.1016/j.jssc.2017.10.018.

[5] S. Shakir, M. Abd-ur-Rehman, K. Yunus, and M. Iwamoto, "Fabrication of un-doped and magnesium

doped TiO2 films by aerosol assisted chemical vapor deposition for dye sensitized solar cells," *J. Alloy. Compd. J.*, vol. 737, pp. 740–747, 2018, doi: 10.1016/j.jallcom.2017.12.165.

[6] A. J. Maira, K. L. Yeung, C. Y. Lee, P. L. Yue, and C. K. Chan, "Size Effects in Gas-Phase Photo-oxidation of Trichloroethylene Using Nanometer-Sized TiO2 Catalysts," vol. 196, pp. 185–196, 2000, doi: 10.1006/jcat.2000.2838.

[7] L. Lu, X. Xia, J. K. Luo, and G. Shao, "Mn-doped TiO 2 thin films with significantly improved optical and electrical properties," vol. 485102, doi: 10.1088/0022-3727/45/48/485102.

[8] A. V Emeline, V. N. Kuznetsov, V. K. Rybchuk, and N. Serpone, "Visible-Light-Active Titania Photocatalysts : The Case of N-Doped TiO2s — Properties and Some Fundamental Issues," vol. 2008, 2008, doi: 10.1155/2008/258394.

[9] T. Umebayashi, T. Yamaki, H. Itoh, and K. Asai, "Band gap narrowing of titanium dioxide by sulfur doping," vol. 454, no. 2002, pp. 3–6, 2012, doi: 10.1063/1.1493647.

[10] M. Devi and M. R. Panigrahi, "Effect of annealing temperature on the optical and electrical properties of Mg doped TiO 2 thin films," vol. 10, pp. 63–74, 2017.

[11] J. Gong, J. Liang, and K. Sumathy, "Review on dye-sensitized solar cells (DSSCs): Fundamental concepts and novel materials," *Renew. Sustain. Energy Rev.*, vol. 16, no. 8, pp. 5848–5860, 2012, doi: 10.1016/j.rser.2012.04.044.

[12] D. Szczuko, J. Werner, S. Oswald, G. Behr, and K. Wetzig, "XPS investigations of surface segregation of doping elements in SnO 2," vol. 179, pp. 1–6, 2001.

[13] Y. Sui *et al.*, "Investigation of Optimum Mg Doping Content and Annealing Parameters of Cu2MgxZn1−xSnS4 Thin Films for Solar Cells," *nanomaterials*, vol. 9, pp. 1–13, 2019, doi: doi:10.3390/nano9070955.

[14] C. Vigreux, B. Deneuve, J. El Fallah, and J. M. Haussonne, "Effects of acceptor and donor additives on the properties of MgTiO3 ceramics sintered under reducing atmosphere," vol. 21, pp. 1681–1684, 2001.

[15] V. Yuniar and E. Yufita, "Structural and optical properties of MgO- doped TiO 2 prepared by sol-gel method Structural and Optical Properties of MgO-doped TiO 2 Prepared by Sol-Gel Method," vol. 110007, no. March, 2020.

[16] U. Singh, L. Bhattacharyya, S. Kumar, R. Mishra, G. Sharma and S. Singh, G. Ahalawat, "Sol-Gel processing of silica nanoparticles and their applications," *Adv. Colloid Interface Sci.*, vol. 214, pp. 17–37, 2014, doi: 10.1016/j.cis.2014.10.007.

[17] M. R. S. Bernadsha,V. Samson, N. Simi, J. Madhavan, "Analyzing the efficiency of nanostructured Sm 3+- and Gd3+- doped TiO2 and constructing DSSCs using efficacious photoanodes," *J. Mater. Sci. Mater. Electron.*, vol. 33, no. 9, pp. 6446–6455, 2022, doi: 10.1007/s10854-022-07816-7.

[18] B. Ünlü and M. Özacar, "Effect of Cu and Mn amounts doped to TiO2 on the performance of DSSCs," *Sol. Energy*, vol. 196, pp. 448–456, Jan. 2020, doi: 10.1016/J.SOLENER.2019.12.043.

[19] A. Aboulouard *et al.*, "Dye sensitized solar cells based on titanium dioxide nanoparticles synthesized by flame spray pyrolysis and hydrothermal sol-gel methods: A comparative study on photovoltaic performances," *J. Mater. Res. Technol.*, vol. 9, no. 2, pp. 1569–1577, 2020, doi: 10.1016/j.jmrt.2019.11.083.

[20] T. S. Bramhankar *et al.*, "Effect of Nickel–Zinc Co-doped TiO2 blocking layer on performance of DSSCs," *J. Alloys Compd.*, vol. 817, p. 152810, Mar. 2020, doi: 10.1016/J.JALLCOM.2019.152810.

[21] M. Geetha *et al.*, "Preparation and characterisation of tailored TiO2 nanoparticles photoanode for dye sensitised solar cells To cite this version : HAL Id : hal-03108287 I NTERNATIONAL J OURNAL OF Preparation and Characterisation of Tailored TiO 2 nanoparticles Photoanode f," 2021.

[22] A. K. Gupta, P. Srivastava, and L. Bahadur, "Improved performance of Ag-doped TiO2 synthesized by modified sol–gel method as photoanode of dye-sensitized solar cell," *Appl. Phys. A Mater. Sci. Process.*, vol. 122, no. 8, pp. 1–13, 2016, doi: 10.1007/s00339-016-0241-2.

[23] A. Merazga, F. Al-Subai, A. M. Albaradi, A. Badawi, A. Y. Jaber, and A. A. B. Alghamdi, "Effect of sol–gel MgO spin-coating on the performance of TiO2-based dye-sensitized solar cells," *Mater. Sci. Semicond. Process.*, vol. 41, pp. 114–120, Jan. 2016, doi: 10.1016/J.MSSP.2015.08.026.

[24] K. Momma and F. Izumi, "VESTA : a three-dimensional visualization system for electronic and structural analysis," pp. 653–658, 2008, doi: 10.1107/S0021889808012016.

[25] K. Sreedhar and N. Pavaskar, "Synthesis of MgTiO3 and Mg4Nb 2O9 using stoichiometrically excess MgO," *Mater. Lett.*, vol. 53, pp. 452–455, 2002, doi: doi.org/10.1016/S0167-577X(01)00525-0.

[26] L. Borkovska *et al.*, "Optical and structural properties of Mn-doped magnesium titanates fabricated with excess MgO," *Mater. Today Commun.*, vol. 27, 2021, doi: 10.1016/j.mtcomm.2021.102373.

[27] A. A. Elabd, O. A. Elhefnawy, and A. M. El Nahrawy, "RSC Advances A new organic-silica based nanocomposite prepared for spectrophotometric determination of uranyl ions," *RSC Adv.*, vol. 6, pp.

9563–9570, 2016, doi: 10.1039/C5RA21401G.
[28] A. A. Haroun, A. M. El Nahrawy, and P. Maincent, "based nanogels for sustained drug delivery systems," vol. 86, no. 5, pp. 691–700, 2014, doi: 10.1515/pac-2013-1110.
[29] A. El Nahrawy, A. Bakr, B. Hemdan, and A. A. Hammad, "Identification of - Fe3+ co-doped zinc titanate mesostructures using dielectric and antimicrobial activities," *Int. J. Environ. Sci. Technol.*, no. 0123456789, 2020, doi: 10.1007/s13762-020-02786-x.
[30] A. El Nahrawy, A. Abou Hammad, and A. Mansour, "Compositional Effects and Optical Properties of P2O5 Doped Magnesium Silicate Mesoporous Thin Films," *Arab. J. Sci. Eng.*, 2020, doi: 10.1007/s13369-020-05067-4.
[31] A. El-Nahrawy, A, Ali, A. Abou Hammad, A. Youssef, "Influences of Ag-NPs doping chitosan/calcium silicate nanocomposites for optical and antibacterial activity," *Int. J. Biol. Macromol.*, 2016, doi: 10.1016/j.ijbiomac.2016.08.045.
[32] Y. Caglar, M. Caglar, and S. Ilican, "Microstructural , optical and electrical studies on sol gel derived ZnO and ZnO : Al fi lms," *Curr. Appl. Phys.*, vol. 12, no. 3, pp. 963–968, 2012, doi: 10.1016/j.cap.2011.12.017.
[33] M. N. An, S. Radiman, N. M. Huang, and M. A. Yarmo, "Sol – gel hydrothermal synthesis of bismuth – TiO 2 nanocubes for dye-sensitized solar cell," vol. 36, pp. 2215–2220, 2010, doi: 10.1016/j.ceramint.2010.05.027.
[34] A. Mansour, A. Abou Hammad, and A. El Nahrawy, "Nano-Structures & Nano-Objects Sol – gel synthesis and physical characterization of novel photodiode," *Nano-Structures & Nano-Objects*, vol. 25, p. 100646, 2021, doi: 10.1016/j.nanoso.2020.100646.